An epi-allelic series of p53 hypomorphs created by stable RNAi produces distinct tumor phenotypes *in vivo*

Michael T. Hemann[1], Jordan S. Fridman[1], Jack T. Zilfou[1], Eva Hernando[2], Patrick J. Paddison[1], Carlos Cordon-Cardo[2], Gregory J. Hannon[1] & Scott W. Lowe[1]

Published online 3 February 2003; doi:10.1038/ng1091

The application of RNA interference (RNAi) to mammalian systems has the potential to revolutionize genetics and produce novel therapies. Here we investigate whether RNAi applied to a well-characterized gene can stably suppress gene expression in hematopoietic stem cells and produce detectable phenotypes in mice. Deletion of the *Trp53* tumor suppressor gene greatly accelerates *Myc*-induced lymphomagenesis, resulting in highly disseminated disease[1,2]. To determine whether RNAi suppression of *Trp53* could produce a similar phenotype, we introduced several *Trp53* short hairpin RNAs (shRNAs) into hematopoietic stem cells derived from Eμ-Myc transgenic mice, and monitored tumor onset and overall pathology in lethally irradiated recipients. Different *Trp53* shRNAs produced distinct phenotypes *in vivo*, ranging from benign lymphoid hyperplasias to highly disseminated lymphomas that paralleled *Trp53*$^{-/-}$ lymphomagenesis in the Eμ-Myc mouse. In all cases, the severity and type of disease correlated with the extent to which specific shRNAs inhibited p53 activity. Therefore, RNAi can stably suppress gene expression in stem cells and reconstituted organs derived from those cells. In addition, intrinsic differences between individual shRNA expression vectors targeting the same gene can be used to create an 'epi-allelic series' for dissecting gene function *in vivo*.

RNAi is a powerful tool for manipulating gene expression in model organisms and cultured mammalian cells[3]. The technology arose from the observation that exogenous double-stranded RNAs induce gene silencing in plants and *Caenorhabditis elegans*. These double-stranded RNAs are processed into small interfering RNAs (siRNAs), which are incorporated into a conserved cellular machinery that mediates the suppression of homologous genes. Recently, small non-coding RNAs have been identified that can act as endogenous regulators of gene expression. These microRNAs typically form stem-loop structures, essentially short double-stranded RNAs, that enter the RNAi pathway[4–7]. shRNAs, modeled after microRNAs, can be expressed from viral vectors to induce stable suppression of gene expression in cultured mammalian cells[8].

We reasoned that stable suppression of gene expression by RNAi should recapitulate the phenotype of mice harboring deletions of the targeted gene. To test this, we targeted the *Trp53* tumor suppressor, a gene with extensively characterized loss-of-function

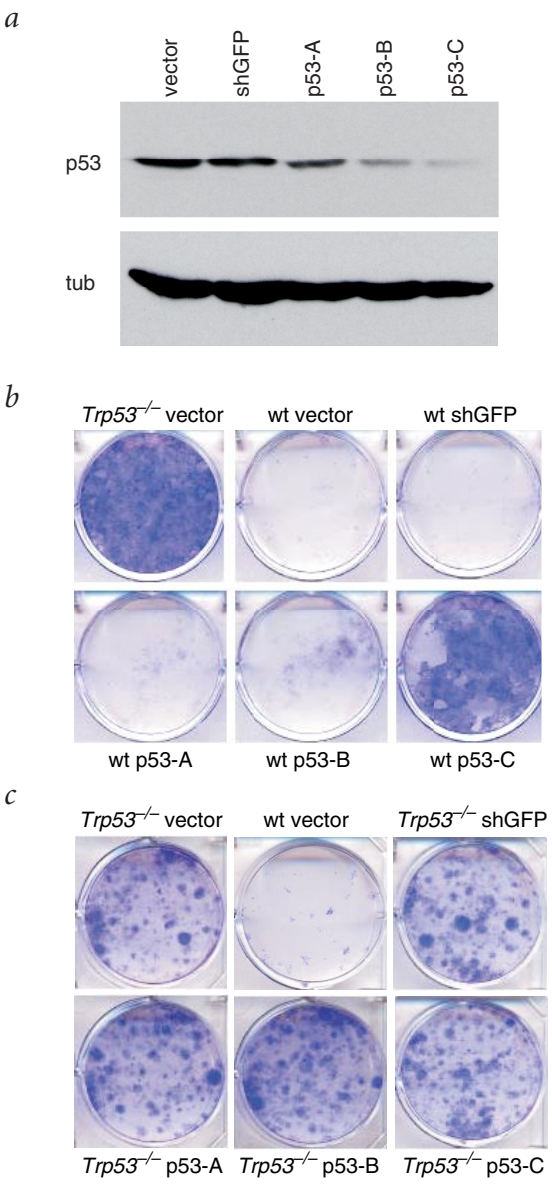

Fig. 1 Analysis of *Trp53* shRNA function *in vitro*. ***a***, Western blot showing the lower p53 levels in H1299 cells transiently transfected with different *Trp53* shRNA retroviral vectors. Tubulin (tub) expression shows equal loading of all samples. ***b***, Colony-formation assay on wild-type (wt) MEFs infected with an empty vector (vector), a vector expressing a nonspecific shRNA (shGFP) and vectors expressing the indicated *Trp53* shRNAs. *Trp53*$^{-/-}$ MEFs infected with an empty vector (vector) are shown as a control. A total of 5,000 cells were plated per well and cultured for 2 wk before staining with crystal violet. ***c***, Colony-formation assay on *Trp53*$^{-/-}$ MEFs infected with control and p53 shRNAs. A total of 1,000 cells were plated per well and analyzed as in *b*. Wild-type (wt) MEFs infected with an empty vector (vector) are shown as a control.

[1]*Cold Spring Harbor Laboratory, Watson School of Biological Sciences, Cold Spring Harbor, New York 11724, USA.* [2]*Department of Pathology, Memorial Sloan Kettering Cancer Center, New York, New York, USA. Correspondence should be addressed to G.J.H. (e-mail: hannon@cshl.org) or S.W.L. (e-mail: lowe@cshl.org).*

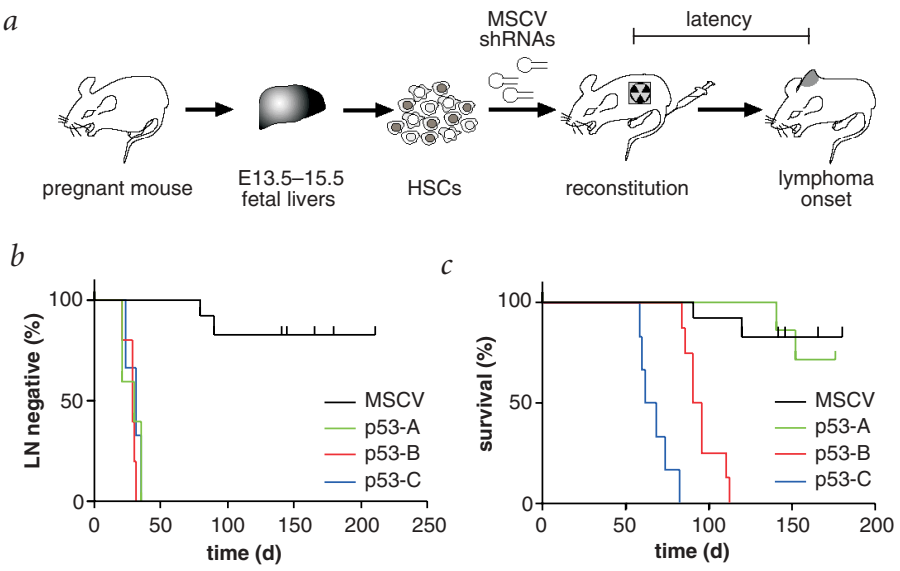

Fig. 2 Acceleration of Eμ-Myc–induced lymphomagenesis by *Trp53* shRNAs. ***a***, Protocol for adoptive transfer experiments using Eμ-Myc hematopoietic stem cells infected with shRNA vectors. ***b***, Mice reconstituted with stem cells infected with the indicated *Trp53* shRNAs were monitored for lymph node enlargement by regular palpation of the axillary, brachial and inguinal nodes. The data are presented in a Kaplan-Meier format showing the percentage of mice that remained free of enlarged lymph nodes at various times after reconstitution (time 0). All mice receiving *Trp53* shRNAs showed lymph node hyperplasia 3–5 wk after injection, whereas control vector recipients did not. ***c***, The animals described in *b* were monitored for tumor onset and illness until they reached a terminal stage and were killed. The data are presented in a Kaplan-Meier format showing overall survival at various times after reconstitution. The p53-B and p53-C, but not p53-A, constructs accelerate lymphomagenesis in recipient animals.

phenotypes[9]. The protein p53 encoded by *Trp53* promotes apoptosis in response to hyperproliferative signals; therefore, p53 inactivation accelerates tumorigenesis initiated by mitogenic oncogenes[10] . For example, Eμ-Myc transgenic mice express the *Myc* oncogene from an immunoglobulin heavy-chain enhancer and develop B-cell lymphomas by 4–6 months of age[11]. However, Eμ-Myc lymphomas harboring *Trp53* deletions arise much earlier, and display a characteristic disseminated pathology[1,2]. Hematopoietic stem cells from Eμ-Myc transgenic mice also give rise to lymphomas upon adoptive transfer into normal recipients, and these lymphomas are greatly accelerated by loss of *Trp53* or by anti-apoptotic genes introduced *ex vivo*[2]. Accordingly, stable suppression of p53 in Eμ-Myc hematopoietic stem cells by RNAi should accelerate lymphomagenesis in recipient animals.

We generated several retroviral vectors containing shRNAs targeting the tumor suppressor *Trp53*, designated p53-A, p53-B and p53-C (see Supplementary Fig. 1 online), and assessed their ability to influence p53 levels and activity. Transient transfection of these shRNA vectors into cultured cells resulted in varying levels of p53 suppression: p53-C achieved the greatest reduction in p53 levels, followed by p53-B and p53-A (Fig. 1*a*). Notably, a control GFP hairpin known to enter the RNAi pathway had no effect on p53 expression.

Colony-formation assays using mouse embryonic fibroblasts (MEFs) infected with these retroviruses also revealed differences among the *Trp53* shRNA vectors (Fig. 1*b*). In this assay, p53 deficiency results in a greatly enhanced ability of untransformed cells to form colonies when plated at clonogenic density. Consistent

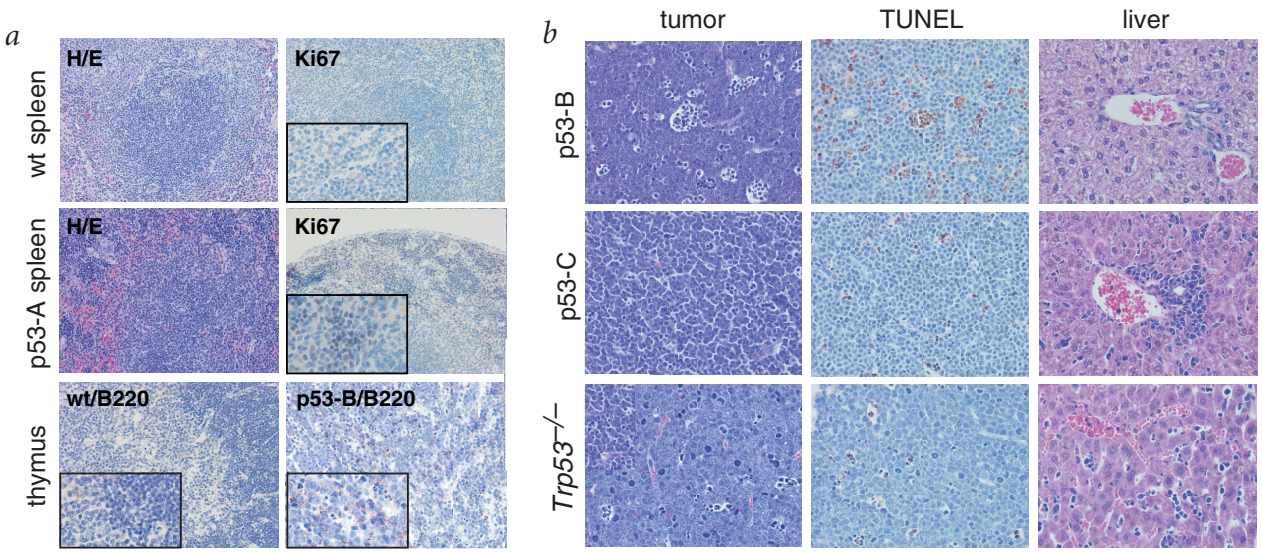

Fig. 3 *Trp53* shRNAs produce distinct pathologies *in vivo*. ***a***, Top, p53-A recipients show splenic hyperplasia. Spleen sections from a normal control and a p53-A recipient, isolated at day 50 after stem cell transplantation, are shown. The p53-A spleen shows a prominent white pulp and increased Ki67 staining (brown) relative to controls. Bottom, Mediastinal lymphomas in p53-B recipients compromise the normal thymic architecture. Whereas a wild-type (wt) thymus shows little B220 staining, the p53-B thymus is completely overtaken by B220-positive lymphoma cells. ***b***, H&E and TUNEL staining of p53-B, p53-C and *Trp53*$^{-/-}$ lymphoma and liver sections. H&E and TUNEL staining of lymphoma sections show clusters of apoptotic cells in p53-B tumors, whereas p53-C and *Trp53*$^{-/-}$ tumors show a relative lack of apoptotic cells. Liver sections from animals harboring p53-B lymphomas do not contain lymphoma cells, whereas livers from mice harboring p53-C and *Trp53*$^{-/-}$ lymphomas show perivascular and parenchymal infiltration of tumor cells.

with the varied abilities of the shRNAs to reduce p53 levels, p53-C produced the greatest colony formation, followed by p53-B and p53-A. None of the p53 shRNAs altered colony formation when expressed in *Trp53*$^{-/-}$ MEFs, indicating that these retroviruses probably have no off-target activities.

Viruses produced from the MSCV control and the p53-A, p53-B and p53-C retroviral vectors were used to infect hematopoietic stem cells isolated from Eμ-Myc fetal livers, and the infected cells were transplanted into lethally irradiated recipient mice (Fig. 2*a*). Whereas mice reconstituted with MSCV transduced (control) stem cells showed no initial signs of proliferative disease, mice reconstituted with stem cells expressing each *Trp53* shRNA vector had palpable lymph nodes 3–5 weeks after stem cell replacement (Fig. 2*b*). Despite this similarly timed onset of lymph node hyperplasia, the three *Trp53* shRNA vectors produced markedly different outcomes (Fig. 2*c*). Mice reconstituted with stem cells infected with p53-A, designated p53-A recipients, showed no decrease in overall survival relative to MSCV controls. In contrast, 8/8 p53-B and 6/6 p53-C recipients developed B-cell lymphomas and reached a terminal stage after an average of 95.0 ± 10.7 and 66.8 ± 9.4 days, respectively ($P < 0.001$ comparing MSCV controls to both p53-B and p53-C and $P < 0.05$ comparing p53-B to p53-C). Therefore, RNAi can suppress *Trp53* in hematopoietic stem cells, resulting in accelerated tumor phenotypes *in vivo*.

Pathological analysis showed marked differences between p53-A, p53-B and p53-C recipients. p53-A recipients showed lymph node enlargement, along with splenic hyperplasia as measured by Ki67 staining (Fig. 3*a*). But these mice did not develop lymphomas at an accelerated rate relative to MSCV controls ($P = 0.8$). The p53-B recipients developed small tumors throughout the lymphatic system and massive lymphomas surrounding and infiltrating the thymus, compromising the normal thymic architecture (Fig. 3*a*). These lymphomas could be transplanted into recipient animals, indicating that they were true malignancies and not severe hyperplasia (data not shown). The p53-B lymphomas showed high levels of apoptosis, a low mitotic index and only minor infiltration into the lung and liver (Fig. 3*b* and data not shown). In contrast, p53-C recipients were markedly similar to mice bearing *Trp53*-null lymphomas, showing only moderately enlarged mediastinal nodes but large disseminated lymphomas. In addition, p53-C tumors had low levels of apoptosis, a high mitotic index and massive lung, liver and spleen infiltration (Fig. 3*b* and data not shown). Therefore, different shRNAs targeting *Trp53* can elicit distinct phenotypes in recipient animals, such that the severity of the resulting tumor phenotype correlates with their ability to reduce p53 levels *in vitro*.

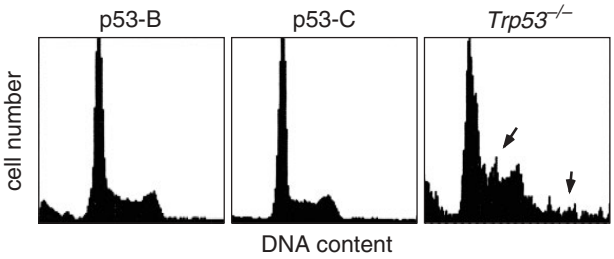

Fig. 4 *Trp53* shRNAs and chromosomal instability. p53-B and p53-C shRNAs lymphomas were compared to a *Trp53*$^{-/-}$ (p53-negative) lymphoma by DNA content analysis. The *Trp53*$^{-/-}$ lymphoma shows cells with abnormal DNA content (black arrows), whereas the tumors produced using *Trp53* shRNAs remain largely diploid. The results are representative of three tumors of each class.

Although lymphomas arising in p53-C shRNA recipients were similar to *Trp53*$^{-/-}$ lymphomas on pathological analysis, analysis of cellular DNA content showed substantial differences. As previously reported, *Trp53*$^{-/-}$ tumor cells were highly aneuploid[2]. In contrast, neither p53-B nor p53-C tumor cells had aberrant DNA content profiles (Fig. 4). These data indicate that the residual p53 levels in p53-B and p53-C tumor cells can preserve chromosome stability but cannot efficiently mediate apoptosis. Although further studies will be needed to determine precisely how different

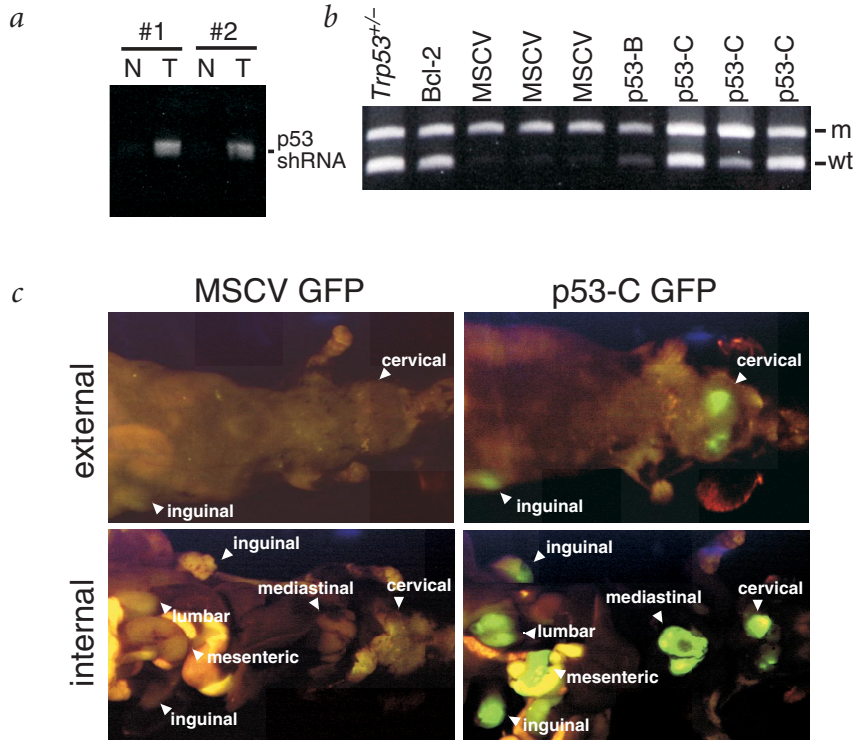

Fig. 5 *Trp53* shRNAs contribute to lymphomas and suppress mutations in endogenous *Trp53*. ***a***, PCR analysis shows that the shRNA construct is present in tumor cells. Genomic DNA was isolated from normal (N) and tumor (T) cells from lymphoma-bearing mice and amplified using primers specific for the U6 promoter–hairpin cassette. Two examples are shown. ***b***, *Trp53* shRNAs prevent LOH of *Trp53* in lymphomas arising from *Trp53*$^{+/-}$ cells. Normal DNA from a *Trp53*$^{+/-}$ mouse (left lane) and tumor DNA from mice harboring stem cells transduced with the indicated vector were subjected to allele-specific PCR to identify the mutant (m) and wild-type (wt) *Trp53* alleles. Owing to selection against p53 function, tumors derived from mice injected with *Trp53*$^{+/-}$ stem cells containing MSCV vector show LOH. In contrast, tumors derived from mice receiving stem cells containing *Trp53* shRNAs show retention of the wt allele. As previously shown[2], Bcl-2 also prevents LOH of *Trp53* in this setting. ***c***, Detection of GFP in tumors arising from *Trp53*$^{+/-}$ stem cells containing a *Trp53* shRNA co-expressed with GFP. External and internal images of the ventral side of tumor-bearing mice are shown. GFP expression indicates the presence of the vector in the resulting lymphoma. Although an MSCV GFP control vector does not enhance lymphomagenesis in *Trp53*$^{+/-}$ cells, the p53-C GFP vector is present in all resulting lymphomas.

degrees of p53 suppression affect p53 effector functions, these results underscore the importance of the apoptotic activity of p53 in suppressing *Myc*-induced lymphomagenesis[2].

We used PCR analysis to confirm the presence of the hairpin construct in accelerated tumors. As expected, 6/6 primary p53-B and p53-C tumors tested contained the MSCV hairpin construct (Fig. 5*a* and data not shown). The constructs were also detected in transplanted tumors, eliminating the possibility that the amplified band arose from non-malignant stem cell–derived cells present in the primary tumors.

Although spontaneous *Trp53* mutations occur in only 10–15% of Eμ-Myc lymphomas, 100% of *Trp53*$^{+/-}$ Eμ-Myc mice develop tumors resulting from loss of heterozygosity (LOH) at the *Trp53* locus[1]. Because the selective pressure to undergo LOH in this context is so high, *Trp53*$^{+/-}$ Eμ-Myc stem cells can serve as an acutely sensitive system for testing whether *Trp53* shRNAs can impair p53 function. Given that *Trp53* shRNAs impair p53 function in other assays, we predicted that RNAi suppression of *Trp53* would allow a proportion of the final tumor mass derived from Eμ-Myc *Trp53*$^{+/-}$ stem cells to develop without LOH of *Trp53*. To test this prediction, we introduced MSCV control, p53-B and p53-C retroviral vectors into *Trp53*$^{+/-}$ Eμ-Myc hematopoietic stem cells and allowed lymphomas to form after adoptive transfer into recipient mice. As previously shown, all tumors derived from *Trp53*$^{+/-}$ stem cells infected with the MSCV vector showed LOH on allele-specific PCR (Fig. 5*b*). In contrast, 1/2 tumors derived from *Trp53*$^{+/-}$ cells containing p53-B and 4/4 tumors derived from *Trp53*$^{+/-}$ cells containing p53-C developed tumors that retained the wild-type *Trp53* allele (Fig. 5*b* and data not shown). Thus, LOH is not necessary for tumor development in the presence of a *Trp53* shRNA.

We visualized *in vivo* the contribution of *Trp53* shRNAs to tumorigenesis by introducing p53-C using a retroviral vector that co-expressed GFP (Fig. 5*c*), which allowed tracking of infected cells by whole-body imaging[2]. Tumors arising in mice that had received *Trp53*$^{+/-}$ Eμ-Myc stem cells infected with this p53-C GFP vector were GFP positive and retained the wild-type *Trp53* allele (Fig. 5*c* and data not shown), whereas lymphomas arising from stem cells infected with MSCV GFP alone were GFP negative and had lost the wild-type *Trp53* allele. Thus, *Trp53* shRNAs promote tumor development by abrogating the requirement for *Trp53*$^{+/-}$ cells to delete the wild-type *Trp53* allele during lymphomagenesis.

Our results have broad implications for mammalian genetics and the use of RNAi as a therapeutic tool. First, they establish stable RNAi as an alternative to homologous recombination for producing loss-of-function phenotypes in mice. Previously, such analyses required the generation of germline mutations. Although homologous recombination remains the only technique for producing complete gene deficiencies, combining stable RNAi with stem cell–based reconstitution of target organs is much more rapid and circumvents the complications that arise from the presence of nullizygous mutations during embryogenesis. Second, our results indicate that shRNAs with intrinsically different abilities to suppress a target gene *in vitro* conserve these relative biological activities *in vivo*. This permits the construction of an epi-allelic series of hypomorphic mutations that, in the case of the *Trp53* shRNAs, produces distinct types of hyperplastic diseases based on differing strengths of p53 suppression. Tumor suppressors often act as components of complex networks, the overall function of which can be impaired by many different genetic or epigenetic alterations. The ability to dampen such networks to different degrees will be of enormous value in studying early stages of disease, which are neither easily nor quickly recapitulated using germline genetic alterations. Finally, our studies provide strong support for the notion that stable RNAi suppression of deleterious genes might be used in therapeutic regimens for human diseases in which stem cells are modified *ex vivo* and then re-introduced into the affected individual.

Methods

Retroviral vectors. We generated retroviruses encoding shRNAs expressed from the U6 promoter by PCR using a pGEM U6 promoter template as previously described[8]. The amplification reactions used a universal 5′ primer corresponding to the SP6 site at the 5′ end of the U6 promoter cassette and a long 3′ primer complementary to the 3′ end of the promoter followed by sequences encoding the *Trp53* shRNA and a pol III termination site. We designed the shRNA sequences using designated software found at the RNAi OligoRetriever Database and encoded inverted repeats of 27–29 bp separated by an 8-nt spacer. The inverted repeats corresponded to nt 266–293 (shp53.1) or 44–72 (shp53.2) of the mouse *Trp53* cDNA, and had at least 3-nt differences from any other murine genes as determined by BLAST. We cloned the resulting PCR products directly into a pENTR/TOPO-D vector (Invitrogen) and then transferred the U6-shRNA cassette to one of several retroviral vectors containing a 'Gateway destination cassette' (Invitrogen) in either the *Nhe*I site of pBabePuro or the *Hpa*I site of MSCV. Altogether, we produced the following retroviral vectors: pBabe p53-A, encoding the shp53.1 hairpin in the 3′ LTR of pBabePuro[8]; pMSCV p53-B, encoding the shp53.1 hairpin 5′ of the PGK-Puro construct encoded by pMSCVpuro (Clontech); pMSCV p53-C, encoding the shp53.2 hairpin 5′ of the PGK-Puro construct encoded by pMSCVpuro; pMSCV GFP, encoding IRES-GFP 3′ of the PGK-Puro construct encoded by pMSCVpuro; and pMSCV p53-C GFP, encoding the shp53.2 hairpin 5′ of the PGK-Puro-IRES-GFP encoded by pMSCV GFP. Cloning strategies and primer sequences are available from the authors on request.

Suppression of p53 levels and activity by *Trp53* shRNAs. We co-transfected H1299 human lung adenocarcinoma cells with plasmids encoding *Trp53* and different *Trp53* shRNAs at a 1:5 ratio using the Fugene reagent (Roche); 36–48 h later, we extracted cells in RIPA buffer (50 mM Tris pH 7.4; 150 mM NaCl; 1% Triton X-100; 0.1% SDS; and 1% sodium deoxycholate) supplemented with Complete Mini protease inhibitors (Roche). We assessed p53 expression by immunoblotting using 50 μg of total cell lysate and an enhanced chemiluminescence (ECL) detection system as described[12], with primary antibodies directed against p53 (1:1,000; CM5, NovoCastra) or α-tubulin (1:2,000; B-5-1-2, Sigma).

We assessed the impact of various *Trp53* shRNAs on p53 function and 'off-target' activities using a colony-formation assay in MEFs. We obtained wild-type and *Trp53*$^{-/-}$ MEFs from embryonic day 13.5 (E13.5) embryos and infected these cells with retroviruses co-expressing various shRNAs and a puromycin-resistance marker (*puro*) as described[13]. We incubated the resulting cell populations for 48 h in the presence of 2 μg/ml puromycin and then plated them at low density in 6-well plates. Two weeks later, the colonies were visualized by crystal violet staining.

RNAi of *Trp53* in stem cells. We isolated, infected and transplanted hematopoietic stem cells exactly as described[2]. We crossbred Eμ-Myc transgenic mice[11] to wild-type (*Trp53*$^{+/+}$) or *Trp53*$^{+/-}$ C57BL/6 mice (Jackson Laboratory) and obtained hematopoietic stem cells from E13.5–15.5 fetal livers. We maintained all mice in the C57BL/6 background and confirmed all stem cell genotypes by PCR. We cultured Eμ-Myc *Trp53*$^{+/+}$ and Eμ-Myc *Trp53*$^{+/-}$ fetal liver cells under conditions that support stem cell proliferation and infected the cells with various shRNA-expressing retroviruses exactly as described[2]. Under these conditions we typically infected 5–15% of fetal liver cells. Then, 36 h later, we used 1×10^6 cells to reconstitute the hematopoietic compartment of lethally irradiated mice (approximately 9 Gray per mouse). The Cold Spring Harbor Animal Care and Use Committee approved all mouse experiments included in this work.

Lymphoma monitoring and analysis. We monitored reconstituted animals for illness by lymph node palpation, by monitoring overall morbidity and, in some cases, by whole-body fluorescence imaging[2]. We assessed the onset of lymph node hyperplasia by regular palpation of the axillary, brachial and inguinal lymph nodes. We defined overall survival as the time from stem cell reconstitution until the animal reached a terminal stage and

had to be killed. In all cases, terminal animals harbored large tumor burdens. We did statistical analysis using a one-way ANOVA test using Graph Pad Prism version 3.0 (Graph Pad Software).

We confirmed the presence of the *Trp53* hairpin in Eμ-Myc lymphomas by PCR amplification of lymphoma DNA with the primers used in generating the U6 promoter–shRNA constructs. We used DNA derived from the infected stem cell populations of the same mouse as a normal control. In experiments using MSCV GFP (control) or MSCV p53-C GFP retroviruses, we used whole-body fluorescence imaging of GFP to monitor the presence of transduced cells in the resulting lymphomas. We carried out external imaging on live mice, and we carried out internal imaging immediately after mice were killed. We determined the occurrence of LOH at the *Trp53* locus in lymphomas derived from $Trp53^{+/-}$ cells by allele-specific PCR of tumor DNA to identify the mutant (targeted) and wild-type *Trp53* alleles[2].

Histopathology. We fixed tissue samples in 10% buffered formalin and embedded them in paraffin, then stained sections (5 μm) with hematoxylin and eosin (H&E) according to standard protocols. For detection of p53 and Ki67, we deparaffinized, rehydrated and processed representative sections in graded alcohols using the avidin–biotin immunoperoxidase method. Briefly, we submitted sections to antigen retrieval by microwave oven treatment for 15 m in 10 mM sodium citrate buffer (pH 6.0). We incubated slides first in 10% normal goat serum for 30 m and then overnight at 4 °C with appropriately diluted primary antibody (rabbit antibody CM5 against mouse p53 and rabbit antibody against Ki67, both from NovoCastra). We next incubated the slides with biotinylated goat rabbit-specific immunoglobulins (Vector Laboratories) at 1:500 dilution for 30 m and then with avidin–biotin peroxidase complexes (1:25; Vector Laboratories) for 30 m. We used diaminobenzidine as the chromogen and hematoxylin as the nuclear counterstain. For B220 immunohistochemistry (rat antibody against mouse CD45R/B220–clone RA3-6B2, BD Biosciences, Pharmingen), antigen retrieval was required, and we used a biotinylated antibody against rat as a secondary antibody. We analyzed the apoptotic rate by TUNEL assay according to published protocols[14]. We determined the DNA content of tumor cells by FACS analysis with propidium iodide staining of ethanol-fixed cells as described[2].

URL. Design of shRNA primers from gene accession numbers can be done at the RNAi OligoRetriever Database, which can be reached through G.J.H.'s website at http://www.cshl.edu/public/SCIENCE/hannon.html.

Note: Supplementary information is available on the Nature Genetics website.

Acknowledgments

We thank J. Adams and T. Jacks for providing mice, and C. Rosenthal, M. E. Dudas, and M. S. Jiao for invaluable technical assistance. P.J.P. is an Arnold and Mabel Beckman Fellow of the Watson School of Biological Sciences. G.J.H. is a Rita Allen Foundation Scholar and is supported by an Innovator award from the U.S. Army Breast Cancer Research Program. This work was supported by US National Cancer Institute (NCI) postdoctoral training grants (M.T.H. and J.T.Z.), program project grants (C.C.C., G.J.H. and S.W.L.) from the NCI, and a generous gift from the Ann L. and Herbert J. Siegel Philanthropic Fund.

Competing financial interests

The authors declare that they have no competing financial interests.

Received 19 November 2002; accepted 3 January 2003

1. Schmitt, C.A., McCurrach, M.E., de Stanchina, E., Wallace-Brodeur, R.R. & Lowe, S.W. INK4a/ARF mutations accelerate lymphomagenesis and promote chemoresistance by disabling p53. *Genes Dev.* **13**, 2670–2677 (1999).
2. Schmitt, C.A. *et al*. Dissecting p53 tumor suppressor functions in vivo. *Cancer Cell* **1**, 289–298 (2002).
3. Hannon, G.J. RNA interference. *Nature* **418**, 244–251 (2002).
4. Knight, S.W. & Bass, B.L. A role for the RNase III enzyme DCR-1 in RNA interference and germ line development in Caenorhabditis elegans. *Science* **293**, 2269–2271 (2001).
5. Ketting, R.F. *et al*. Dicer functions in RNA interference and in synthesis of small RNA involved in developmental timing in C. elegans. *Genes Dev.* **15**, 2654–2659 (2001).
6. Hutvagner, G. *et al*. A cellular function for the RNA-interference enzyme Dicer in the maturation of the let-7 small temporal RNA. *Science* **293**, 834–838 (2001).
7. Grishok, A. *et al*. Genes and mechanisms related to RNA interference regulate expression of the small temporal RNAs that control *C. elegans* developmental timing. *Cell* **106**, 23–34 (2001).
8. Paddison, P.J. & Hannon, G.J. RNA interference: the new somatic cell genetics? *Cancer Cell* **2**, 17–23 (2002).
9. Attardi, L.D. & Jacks, T. The role of p53 in tumour suppression: lessons from mouse models. *Cell. Mol. Life Sci.* **55**, 48–63 (1999).
10. Evan, G.I. & Vousden, K.H. Proliferation, cell cycle and apoptosis in cancer. *Nature* **411**, 342–348 (2001).
11. Adams, J.M. *et al*. The c-myc oncogene driven by immunoglobulin enhancers induces lymphoid malignancy in transgenic mice. *Nature* **318**, 533–538 (1985).
12. Zilfou, J.T., Hoffman, W.H., Sank, M., George, D.L. & Murphy, M. The corepressor mSin3a interacts with the proline-rich domain of p53 and protects p53 from proteasome-mediated degradation. *Mol. Cell. Biol.* **21**, 3974–3985 (2001).
13. McCurrach, M.E. & Lowe, S.W. Methods for studying pro- and antiapoptotic genes in nonimmortal cells. *Methods Cell Biol.* **66**, 197–227 (2001).
14. Di Cristofano, A., De Acetis, M., Koff, A., Cordon-Cardo, C. & Pandolfi, P.P. Pten and p27KIP1 cooperate in prostate cancer tumor suppression in the mouse. *Nat. Genet.* **27**, 222–224 (2001).